JB
Journals.ASM.org

AhpC Is Required for Optimal Production of Enterobactin by *Escherichia coli*

Li Ma and Shelley M. Payne

Section of Microbiology and Molecular Genetics and Institute for Cellular and Molecular Biology, University of Texas at Austin, Austin, Texas, USA

***Escherichia coli* alkyl hydroperoxide reductase subunit C (AhpC) is a peroxiredoxin that detoxifies peroxides. Here we show an additional role for AhpC in cellular iron metabolism of *E. coli*. Deletion of *ahpC* resulted in reduced growth and reduced accumulation of iron by cells grown in low-iron media. Liquid chromatography-mass spectroscopy (LC-MS) analysis of culture supernatants showed that the *ahpC* mutant secreted much less enterobactin, the siderophore that chelates and transports ferric iron under iron-limiting conditions, than wild-type *E. coli* did. The *ahpC* mutant produced less 2,3-dihydroxybenzoate, the intermediate in the enterobactin biosynthesis pathway, and providing 2,3-dihydroxybenzoate restored wild-type growth of the *ahpC* mutant. These data indicated that the defect was in an early step in enterobactin biosynthesis. Providing additional copies of *entC*, which functions in the first dedicated step of enterobactin biosynthesis, but not of other enterobactin biosynthesis genes, suppressed the mutant phenotype. Additionally, providing either shikimate or a mixture of *para*-aminobenzoate, tryptophan, tyrosine, and phenylalanine, which, like enterobactin, are synthesized from the precursor chorismate, also suppressed the mutant phenotype. These data suggested that AhpC affected the activity of EntC or the availability of the chorismate substrate.**

The ability to acquire sufficient iron from the environment is essential for growth of most bacteria, including *Escherichia coli*. An efficient mechanism of iron acquisition by *E. coli* under iron-limiting conditions involves the synthesis and secretion of the siderophore enterobactin, a cyclic trimer of 2,3-dihydroxybenzoyl serine (35, 36, 39). This low-molecular-weight, high-affinity chelator sequesters ferric iron and facilitates its transport to the cytoplasm of the cell (35, 36, 39).

There are six genes, *entA* to *-F*, encoding enzymes for enterobactin biosynthesis from the precursor chorismate (7, 49, 50). In the initial stage of enterobactin biosynthesis, the enzymes EntC, EntB, and EntA convert chorismate to 2,3-dihydroxybenzoate (DHB) (27, 28, 44). The remaining enzymes, EntD to -F, together with the bifunctional enzyme EntB, convert DHB to enterobactin, which is secreted by the cells (Fig. 1) (10, 17, 50). Extracellular enterobactin binds ferric iron, and the complex is transported back into the cells via a ligand-specific transport system encoded by *fepABCDG* (4, 23). *E. coli* also has the ability to transport xenosiderophores, including the fungal siderophore ferrichrome (Fc) (5).

The expression of genes encoding iron transport proteins is regulated by the transcriptional repressor Fur (20, 29). Under iron-rich conditions, iron in the cytoplasm binds Fur, and Fe-Fur binds at the promoter regions of iron-responsive genes, repressing their transcription (29). Under iron-limiting conditions, there is insufficient iron available in the cytoplasm to bind Fur, so Fur no longer binds the promoters and transcription is derepressed (29).

In a screen for mutants defective in iron acquisition, we noted that a mutant deleted for genes in both the glutathione and thioredoxin reductase systems (*gor* and *trxB*) had reduced growth under low-iron conditions. These two systems have overlapping functions in maintaining proteins in a reduced state in the cytoplasm (6, 41). While single mutants lacking genes encoding the glutathione reductase (*gor*) or thioredoxin reductase (*trxB*) grow similarly to the wild type in rich medium, the *gor trxB* double mutant grows very poorly and rapidly accumulates suppressor mutations (40). The suppressor mutations were mapped to a gene encoding alkyl hydroperoxide reductase subunit C (AhpC) (40). One frequent suppressor mutation, designated *ahpC**, has a triplet expansion at position 38 in *ahpC* (40), and this mutation was present in the *gor trxB* mutant we tested.

AhpC is a member of the alkyl hydroperoxide reductase system, which in *E. coli* consists of two proteins: a peroxiredoxin (AhpC) and a flavoprotein disulfide reductase (AhpF). AhpC converts peroxides to alcohol and water, and AhpF recycles the oxidized AhpC (22, 48). AhpC is a homodimer and belongs to the 2-Cys peroxiredoxin family, with C46 of one subunit attacking the peroxide substrate, being oxidized to a cysteine sulfenic acid and resolved by C165 of the other subunit (11, 22). Furthermore, the oligomeric states of AhpC correlate with the oxidation-reduction states of AhpC. The reduced form of AhpC is exclusively decameric. Disulfide bond formation results in a loss of stability of the decamer and in dissociation to the dimeric form (53).

Here we show that mutations in *ahpC* affect cellular iron metabolism of *E. coli* and that it is the *ahpC** mutation in the *gor trxB ahpC** mutant that is responsible for reduced growth under low-iron conditions. The participation of AhpC is in an early step in enterobactin biosynthesis, demonstrating a previously uncharacterized role for AhpC.

MATERIALS AND METHODS

Bacterial strains, plasmids, and growth conditions. Strains and plasmids are listed in Table 1, and primer sequences are listed in Table 2. Strains BW25113*ahpF* and BW25113*trxB* were constructed by bacteriophage P1 transduction of the *ahpF* and *trxB* deletion mutations from Keio collection mutants (2) into *E. coli* strain BW25113. To verify that this strain does

Received 25 August 2012 **Accepted** 26 September 2012
Published ahead of print 5 October 2012
Address correspondence to Shelley M. Payne, smpayne@austin.utexas.edu.

doi:10.1128/JB.01574-12

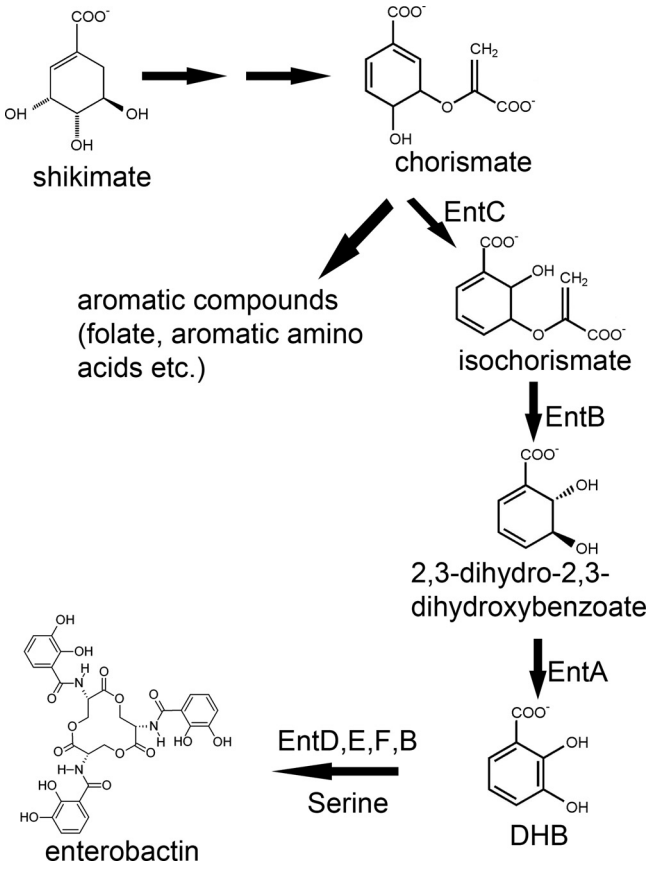

FIG 1 Enterobactin biosynthesis branch of the shikimic acid pathway of *E. coli*. In *E. coli*, enterobactin is synthesized from chorismate, which is derived from the shikimic acid pathway (9). There are six genes, *entA* to *-F*, encoding enzymes for enterobactin biosynthesis in *E. coli*. EntC, the isochorismate synthase, converts chorismate to isochorismate; EntB, the isochorismatase, converts isochorismate to 2,3-dihydro-2,3-dihydroxybenzoate; and EntA, the 2,3-dihydro-2,3-dihydroxybenzoate dehydrogenase, converts 2,3-dihydro-2,3-dihydroxybenzoate to DHB. EntDEF, together with the bifunctional enzyme EntB, converts DHB to enterobactin (50). (Modified from reference 54.)

not carry the *rpoS* mutation found in some related strains, the *rpoS* gene was analyzed by DNA sequencing and confirmed to be the wild-type allele. Strain BW25113*entF* was derived by bacteriophage P1 transduction of the *entF* mutation from ARM110 (33) into BW25113. Strains ML100 and ML300 were derived by introducing the *ahpC* deletion from the *ahpC* mutant of the Keio collection into BW25113 and BW25113*entF* by allelic exchange, as follows. The Δ*ahpC*::kan cassette was amplified from the *ahpC* mutant by use of primers P1 and P2 and Platinum *Pfx* DNA polymerase (Invitrogen, Carlsbad, CA). The product was digested with XbaI and XhoI and cloned into pHM5 (43) digested with XbaI and XhoI. BW25113*gor* was also constructed by allelic exchange. Primers P3 and P4 were used to amplify the Δ*gor*::kan region of the *gor* mutant from the Keio collection for cloning into the EcoRV site of pHM5. pHM5*ahpC* and pHM5*gor* were transformed into DH5αλpir and subsequently introduced into BW25113 by triparental mating (19), and the mutants were isolated as described previously (31). All mutations were confirmed by DNA sequencing.

Strains were cultured in LB or in Tris-buffered minimal medium without added iron (T medium) (45) at 37°C with aeration. T medium contained approximately 0.2 μM iron. Where indicated, LB broth was supplemented with iron (100 μM $FeSO_4$), 1 mM DHB, or 200 μM shikimate, and T medium was supplemented with either iron (10 μM $FeSO_4$) or a mixture of phenylalanine, tryptophan, tyrosine (each at 20 μg/ml), and *para*-aminobenzoic acid (50 μg/ml). The ferric iron chelator ethylenediamine-*N*,*N*′-bis(2-hydroxyphenylacetic acid) (EDDA or EDDHA) (15), deferrated by the method of Rogers (42), was added where indicated.

Antibiotics were used at the following concentrations: ampicillin, 50 μg/ml; chloramphenicol, 30 μg/ml; kanamycin, 50 μg/ml; and tetracycline, 12.5 μg/ml. For growth assays, cultures were inoculated to an initial optical density at 650 nm (OD_{650}) of 0.01 and grown at 37°C with aeration. Growth was monitored by measuring the OD_{650} over 16 h or by diluting and plating cells to determine the number of CFU.

Plasmid construction. To construct pAhpC and pAhpC*, the *ahpC* and *ahpC** genes of strains BW25113 and SMG96, respectively, were amplified with Platinum *Pfx* DNA polymerase, using primers P5 and P6. Each PCR fragment was digested with XbaI and XhoI and inserted into pWSK29 digested with XbaI and XhoI. pEnt1 (*entCEBA*) and pEnt2 (*entC*) were constructed by amplifying the genes from *E. coli* strain BW25113 with Platinum *Pfx* DNA polymerase, using primers P7 and P8 for *entCEBA* and primers P9 and P10 for *entC*. Each PCR fragment was cloned into the EcoRV site of pWSK29. All constructs were confirmed by DNA sequencing.

Site-directed mutagenesis was used to replace each of the two cysteine residues in AhpC with serine. The plasmid $pAhpC^{C46S}$ was constructed by splice overlap extension PCR as described previously (21), using Platinum *Pfx* DNA polymerase and primers P5, P6, P11, and P12. The plasmid $pAhpC^{C165S}$ was constructed using primers P13 and P14 and Phusion Hotstart thermostable proofreading DNA polymerase (NEB, Ipswich, MA), following the QuikChange site-directed mutagenesis protocol (Agilent Technologies, Santa Clara, CA). All constructs were confirmed by DNA sequencing.

Iron metabolism assays. (i) Bioassay. For *ent*-negative strains, 4.8×10^3 CFU/ml of bacterial cells were added to molten LB agar containing 0.2 mg/ml EDDA and allowed to solidify. Iron sources (5 μl) were spotted onto the surface of the agar, and the diameter of the zone of growth around each iron source was measured after 24 h of incubation at 37°C. Iron sources used were 10 μM purified enterobactin (generously provided by K. N. Raymond, University of California, Berkeley, CA), 10^9 cells/ml BW25113 as a source of enterobactin and related catechols, 0.8 mM ferrichrome (Fc) (Sigma, St. Louis, MO), and 25 mM $FeSO_4$.

(ii) Sensitivity assays. To measure sensitivity to iron chelation by EDDA, overnight cultures were diluted 1:600 in 5 ml LB broth containing EDDA at concentrations ranging from 0 to 2.5 mg/ml and grown with aeration at 37°C for 8 h, at which time the OD_{650} was measured.

To measure sensitivity to cumene hydroperoxide, 100-μl overnight cultures of each strain were mixed with 3 ml of LB top agar and poured onto LB plates. Ten microliters of 5% cumene hydroperoxide was spotted on a sterile paper disc that was placed in the center of the plate. After 24 h of incubation at 37°C, the diameters of the killing zones of bacteria were measured.

Detection of catechols and enterobactin. To quantitatively measure extracellular catechol concentrations, overnight cultures in LB broth were centrifuged, and the cells were resuspended in the same volume of saline and then diluted 1:500 in T medium. The cultures were grown with aeration at 37°C for 24 h. Catechols were assayed by a modification of the method of Arnow (1), as follows. The culture was centrifuged, and 0.5 ml of 0.5 N HCl was added to 0.5 ml of supernatant, followed by 0.5 ml of nitrite-molybdate (10% sodium nitrite and 10% sodium molybdate) and 0.5 ml 1 N NaOH. The intensity of the red color, indicative of the presence of catechol, was determined by measuring the absorbance at 515 nm. Samples were normalized to the OD_{650} of the original culture, and the amount of catechol was expressed as 1 Arnow unit, which is equal to $1{,}000 \times OD_{515}/OD_{650}$.

Direct detection of enterobactin in the supernatant was performed by a modification of the method of Furrer et al. (16), as follows. Fifty milliliters of the supernatant was collected and acidified by adding 250 μl of concentrated HCl, followed by extraction with a 1/8 volume of ethyl acetate, twice. The extracts were dried using a SpeedVac system and analyzed

TABLE 1 Strains and plasmids used for this study

Strain or plasmid	Description	Source or reference
Strains		
DHB4	MC1000 [F′ lacI^{q}pro λ$^-$ ΔlacX74 galE galK thi rpsL phoR ΔphoA(PvuII) ΔmalF3]	G. Georgiou; 14
SMG96	DHB4 *gor trxB ahpC**	G. Georgiou; 14
DH5αλpir	F$^-$ Δ(*lacZYA-argF*)*U169 recA1 endA1 hsdR1 supE44 thi-1 gyrA96 relA1* λ::*pir*	24
BW25113	F$^-$ Δ(*araD-araB*)*567* Δ*lacZ4787*(::*rrnB-3*) λ$^-$ *rph-1* Δ (*rhaD-rhaB*)*568 hsdR514*	8
ML100	BW25113 *ahpC*::kan	This work
ML300	BW25113 *ahpC*::kan *entF*::cam	This work
BW25113*ahpF*	BW25113 *ahpF*::kan	This work
BW25113*entF*	BW25113 *entF*::cam	This work
BW25113*gor*	BW25113 *gor*::kan	This work
BW25113*trxB*	BW25113 *trxB*::kan	This work
Plasmids		
pWSK29	Low-copy-number vector; Amp^r	51
pAhpC	*ahpC* in pWSK29	This work
pAhpC*	*ahpC** in pWSK29	This work
pAhpC^{C46S}	*ahpC*^{C46S} in pWSK29	This work
pAhpC^{C165S}	*ahpC*^{C165S} in pWSK29	This work
pCP410	*entEBA* in pACYC184; Tet^r	38
pEnt1	*entCEBA* in pWSK29	This work
pEnt2	*entC* in pWSK29	This work
pHM5	Suicide vector; Amp^r sucrose^s	43
pJS4700	*entF* in pGEMBlue; Amp^r	47
pQF50	Promoterless *lacZ* reporter plasmid; Amp^r	13
pAML23	*ryhB-lacZ* transcriptional fusion in pQF50	32

by liquid chromatography-mass spectrometry (LC-MS) at the University of Texas at Austin Protein and Metabolite Analysis Facility. For LC-MS, the flow rate was 0.15 ml/min and fractions were monitored at a wavelength of 220 nm.

Measurement of total cellular iron content. Overnight LB broth cultures were centrifuged, resuspended in an equal volume of saline, diluted 1:500 in 25 ml LB broth or T medium, and grown with aeration at 37°C for 12 h (LB broth) or 24 h (T medium). A total of 4×10^9 cells from each sample were collected, washed once with saline, and lysed by adding an equal volume of concentrated HNO_3. The homogenized sample was analyzed in an Agilent 7500ce inductively coupled plasma mass spectrometer (ICP-MS) at the University of Texas at Austin School of Geological Sciences.

***In vitro* competition assay.** Overnight cultures of the wild-type (BW25113) and *ahpC* mutant (ML100) strains were centrifuged and resuspended in saline. Equal numbers of cells (1.25×10^8 CFU) of each strain were mixed in 50 ml T medium and grown with aeration at 37°C for 18 h. Each strain (2.5×10^8 CFU) was also grown individually in T medium under the same conditions. Growth was monitored by diluting and plating cells in triplicate on LB agar every 2 h. The growth of the *ahpC* mutant in the mixture was determined by patching the colonies from LB agar to LB agar containing kanamycin, and the growth of the wild type was determined by subtraction of the number of Kan^r colonies from the total.

β-Galactosidase assay. Cells carrying *lacZ* transcriptional fusions were grown with aeration at 37°C for 3 h in LB broth containing EDDA and 50 μg/ml ampicillin. β-Galactosidase was measured as described by Miller (34).

SDS-PAGE and Western immunoblotting. After growing overnight at 37°C with aeration, 1×10^9 bacterial cells were collected by centrifugation, resuspended in 75 μl sodium dodecyl sulfate-polyacrylamide gel electrophoresis (SDS-PAGE) sample buffer, and boiled for 5 min. Five microliters of each sample was loaded onto a 12% polyacrylamide gel. Following electrophoresis, the gels were either stained with Coomassie blue or electroblotted for 1.5 h at 45 V onto Hybond ECL nitrocellulose (Amersham Pharmacia Biotech, Little Chalfont, Buckinghamshire, England). Western immunoblots were incubated with an anti-AhpC rabbit polyclonal primary antibody (generously provided by L. Poole, Wake Forest University School of Medicine) and a horseradish peroxidase (HRP)-conjugated goat anti-rabbit IgG (Bio-Rad Laboratories, Hercules, CA) secondary antibody (diluted 1:10,000). The signal was detected by developing the blot with an enhanced chemiluminescence (ECL) detection kit (Pierce, Rockford, IL).

TABLE 2 Primers used for this study

Primer	Sequence (5′–3′)
P1	CGAGCTCCCAGATCGTCCATCAGTTTCTCATTG
P2	CTCTAGACAGCTTCTGCCCTTCAGTCTTC
P3	GTGTGTAGCATGGGGTTAAGTGT
P4	TCCAGCAATAGCCCGCTT
P5	CTCTAGACAGGCAGGCACTGAAGATACCAAAG
P6	CGAGCTCAGCACCCGAAGAATTAGGTGAATTTCC
P7	AGAAGGGCGTTGCGGTAGAG
P8	CAGTTCGTCGAGCGTTAAATGG
P9	AGAAGGGCGTTGCGGTAGAG
P10	GCCAGCGGGTGAATGGAATG
P11	CGGCTGACTTTACTTTCGTATCCCCGACCGAAC
P12	GTTCGGTCGGGGATACGAAAGTAAAGTCAGCCG
P13	CTTCTCACCCAGGTGAAGTTTCCCCGGCTAAAT
P14	ATTTAGCCGGGGAAACTTCACCTGGGTGAGAAG

RESULTS

Deletion of *ahpC* leads to increased sensitivity to iron chelation. Analysis of a *trxB gor* mutant (SMG96) in the EDDA sensitivity assay indicated that it had increased sensitivity to iron chelation by EDDA compared to its parent strain (Fig. 2A). SMG96 not only carries deletions in the reductase genes *gor* and *trxB* but also carries a suppressor mutation in *ahpC*, which encodes an alkyl hydroperoxidase. This suppressor mutation, designated *ahpC**, has a

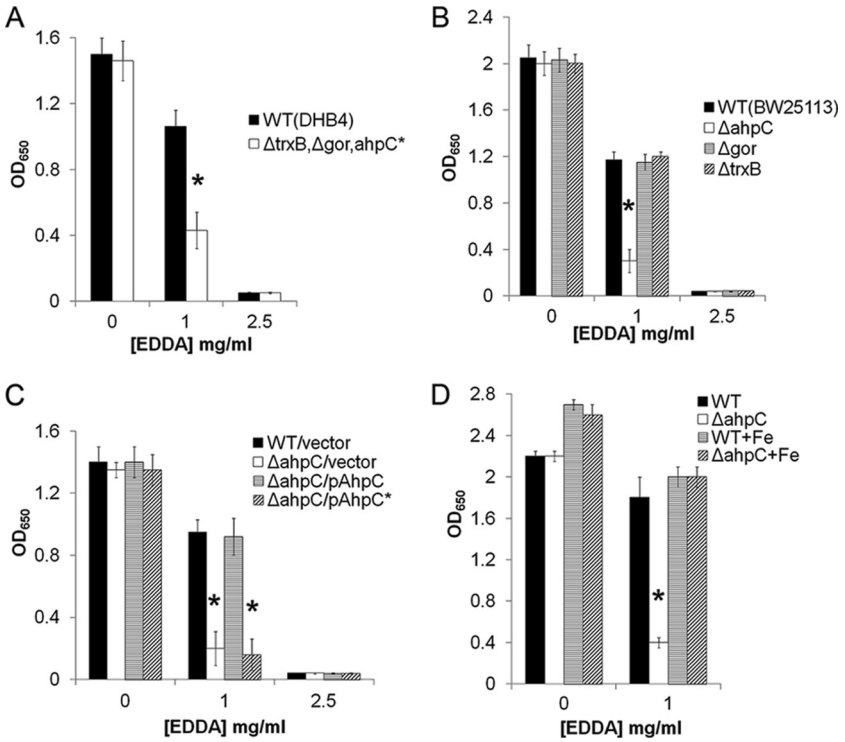

FIG 2 AhpC was required for wild-type growth in low-iron medium. Strains were grown in LB broth containing EDDA for 8 h, and their OD_{650}s were measured. Data presented are averages for at least three independent experiments, and error bars represent 1 standard deviation. *, $P < 0.01$ compared to the wild-type strain, determined by Student's *t* test. (A) The EDDA sensitivity of the *gor trxB ahpC** mutant strain SMG96 was compared to that of its wild-type parent strain, DHB4. (B) EDDA sensitivities of the *ahpC* (ML100), BW25113*gor*, and BW25113*trxB* mutants were compared to that of their wild-type parent, BW25113. (C) The wild-type strain (BW25113) carrying the empty vector (pWSK29) and the *ahpC* mutant (ML100) carrying the empty vector (pWSK29), the wild-type *ahpC* gene (pAhpC), or the *ahpC** gene (pAhpC*) were tested for EDDA sensitivity. (D) The wild-type (BW25113) and *ahpC* (ML100) strains were grown in LB broth containing EDDA, with or without 100 μM added $FeSO_4$.

codon expansion at position 38 that gives the protein reductase activity but eliminates the peroxidase function (39). Therefore, to determine the genetic basis for the reduced fitness of SMG96 under iron-limiting conditions, single deletions in *gor*, *trxB*, and *ahpC* were constructed in strain BW25113, and the resulting mutants were tested for EDDA sensitivity.

Deletion of *ahpC*, but not *gor* or *trxB*, resulted in an increased EDDA sensitivity compared to that of the wild type (Fig. 2B). Wild-type resistance to iron chelation was restored by providing the *ahpC* gene carried on a plasmid (Fig. 2C). However, the *ahpC** gene, which suppressed the *gor trxB* mutant's reductase phenotype, did not suppress the increased EDDA sensitivity of the *ahpC* mutant (Fig. 2C). The *ahpC* mutant carrying pAhpC* was tested by Western blot analysis to confirm that the protein was produced. The results showed that the amount of AhpC* protein produced by that strain was comparable to the level of AhpC detected in the wild-type strain (Fig. 3B). These data indicate that the functional activity of AhpC is required for wild-type resistance to iron chelation and that deletion of *ahpC* or mutation of *ahpC* to *ahpC** results in reduced growth in the presence of an iron chelator.

To confirm that the increased EDDA sensitivity of the *ahpC* mutant was due to iron starvation, the wild type and the *ahpC* mutant were tested in the EDDA sensitivity assay, with or without added iron. In the presence of added iron, the *ahpC* mutant grew to the same level as the wild type (Fig. 2D), confirming that the reduced growth of the *ahpC* mutant in the presence of EDDA was due to iron limitation. The *ahpC* mutant also showed reduced growth in a low-iron minimal medium (T medium). Similarly, the *ahpC* mutant grew more slowly and plateaued at a lower cell density than the wild type in T medium, and the difference was eliminated by addition of iron (Fig. 4).

Internal iron levels are lower in the *ahpC* mutant. To determine whether the reduced growth in low-iron medium indicated that the *ahpC* mutant was more iron starved than the wild type, expression of a reporter plasmid was used as a measure of the internal iron level. The reporter plasmid (32) has a transcriptional fusion of the *ryhB* promoter, which is iron regulated via Fur, with *lacZ*. Thus, transcription of *lacZ* increases as intracellular iron levels decrease. In the presence of EDDA, the β-galactosidase activities were significantly higher in the *ahpC* mutant than in the wild type (Fig. 5), suggesting that the *ahpC* mutant had a lower level of internal iron available to Fur.

To directly measure the total cellular iron levels in the wild type and the *ahpC* mutant, inductively coupled plasma mass spectroscopy was used to measure the iron contents of wild-type and *ahpC* mutant cells under both iron-limiting and iron-rich conditions. The results showed that under iron-limiting conditions, the *ahpC* mutant had a total cellular iron content of 8×10^{-6} μg/10^9 cells, which was reduced relative to the content of 17×10^{-6} μg/10^9 cells measured in the wild type. The total cellular iron contents of the wild type and the *ahpC* mutant were essentially the same under

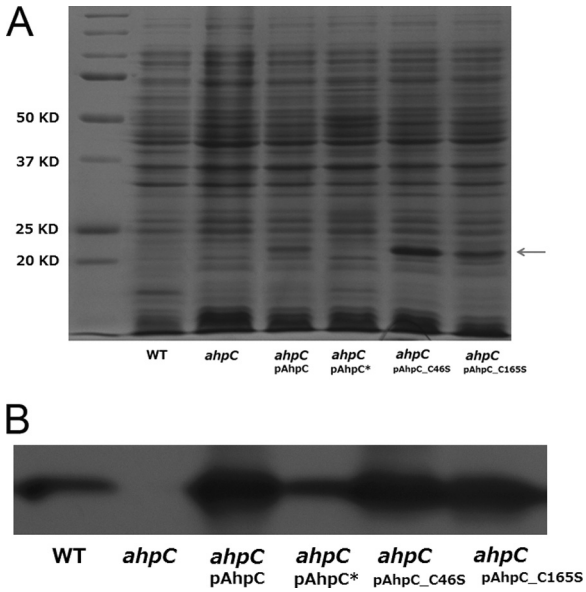

FIG 3 AhpC* and AhpC cysteine mutant proteins were synthesized at wild-type or higher levels. (A) Protein samples from equal numbers of cells (6×10^7) grown to stationary phase were separated in a 12% SDS-PAGE gel and visualized by Coomassie blue staining. AhpC is indicated by an arrow. (B) The wild-type strain (WT) carrying the empty vector (BW25113/pWSK29), the *ahpC* mutant carrying the empty vector (ML100/pWSK29), and the *ahpC* mutant (ML100) carrying plasmids containing wild-type *ahpC* (pAhpC), *ahpC** (pAhpC*), $ahpC^{C46S}$ (pAhpC^{C46S}), or $ahpC^{C165S}$ (pAhpC^{C165S}) were analyzed by Western immunoblotting with anti-AhpC rabbit polyclonal primary antibody and horseradish peroxidase-conjugated goat anti-rabbit IgG secondary antibody.

iron-rich conditions: 87×10^{-6} μg/10^9 cells and 90×10^{-6} μg/10^9 cells, respectively. These data show that AhpC is required to maintain the total cellular iron level under conditions where iron is limiting.

AhpC affects enterobactin production but not enterobactin uptake and utilization. Enterobactin-mediated iron acquisition is a major pathway for *E. coli* to acquire ferric iron under iron-limiting conditions. To determine whether AhpC affected enterobactin production, the extracellular concentration of enterobactin was estimated by the Arnow assay for catechols (1). There was a significant difference in the amounts of extracellular catechols detected between the wild type (35 ± 6 Arnow units) and the *ahpC* mutant (12 ± 5 Arnow units) ($P < 0.01$ by Student's *t* test) when the strains were grown in T medium. The Arnow assay detects total catechols, including enterobactin and some of its precursors and breakdown products. Therefore, LC-MS was used to determine whether there was a difference in the amount of enterobactin produced in the cultures. Supernatants of the wild-type strain showed a peak at 29 min, the expected retention time for enterobactin, whereas the *ahpC* mutant lacked a corresponding peak (Fig. 6A). The fraction containing the peak for the wild-type strain was further analyzed by MS. The *m/z* ratio matched that of enterobactin (Fig. 6B). These data indicate that AhpC is required for wild-type enterobactin biosynthesis or secretion and that most of the catechols detected by the Arnow assay are not enterobactin.

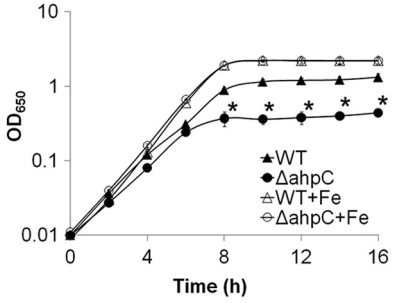

FIG 4 The *ahpC* mutant showed reduced growth in minimal, low-iron medium. The wild-type (BW25113) and *ahpC* mutant (ML100) strains were grown in T medium, with or without added 10 μM $FeSO_4$. Data presented are averages for at least three independent experiments, and error bars represent 1 standard deviation. *, $P < 0.01$ compared to the wild type, determined by Student's *t* test.

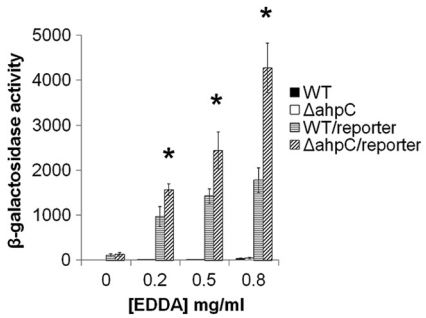

FIG 5 The *ahpC* mutant showed a lower level of internal iron available to Fur upon iron starvation. The strains used were the wild type (BW25113) and the *ahpC* mutant (ML100) containing the empty vector (pQF50) or a *ryhB-lacZ* fusion (pAML23). Strains were grown to early log phase in LB broth containing the indicated concentrations of EDDA, and β-galactosidase activity was measured. Data are expressed in Miller units and are averages for at least three independent experiments ± 1 standard deviation. *, $P < 0.01$ compared to the wild type, determined by Student's *t* test.

To determine if AhpC participates in enterobactin transport or utilization in addition to enterobactin biosynthesis, a competition assay was used. If the defect of the *ahpC* mutant was in transport or utilization of enterobactin, the *ahpC* mutant would be expected to be outcompeted by the wild type, even though both strains would have equal access to the pool of secreted siderophores. To test this, equal numbers of the wild type and the *ahpC* mutant were grown separately or inoculated together in T medium, and their growth was monitored. The *ahpC* mutant showed reduced growth compared to that of the wild type when the strains were grown separately (Fig. 7A). However, when the wild-type and *ahpC* strains were inoculated together, they grew equally well (Fig. 7B). It should be noted that in the mixture, each strain was inoculated at one-half the number of cells used for inoculation of that strain alone, so the total number of cells per ml was the same in each culture. The mixture reached a final density comparable to that of the wild type grown alone, with each strain contributing approximately half the total cell number. This indicates that AhpC is not required for enterobactin transport or utilization.

The *ahpC* mutant was also tested for the ability to use iron sources other than ferri-enterobactin. This was assessed in a bioassay in which the strains were seeded at low density into agar containing an iron chelator and then siderophores or iron was spotted onto the surface of the agar. Both the parent strain and the *ahpC* mutant contained an *entF* mutation to eliminate endogenous enterobactin biosynthesis. The bioassay results showed no

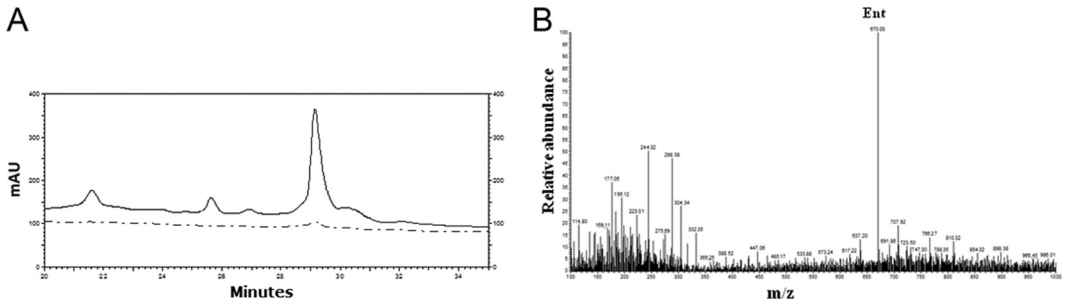

FIG 6 The *ahpC* mutant produced less enterobactin than the wild type. (A) C_{18} chromatography of supernatants of the wild type (solid line) and the *ahpC* mutant (dotted line). (B) Mass spectrometry of the fraction from the wild-type strain containing the peak at 29 min from LC. Enterobactin (molecular weight, 669.55 g/mol) is indicated.

difference in the ability of the *entF* and *ahpC entF* mutants in using ferrichrome, $FeSO_4$, or exogenous enterobactin (Table 3). These data further support the hypothesis that the defect in growth in low-iron medium by the *ahpC* mutant is likely due to its inability to produce sufficient enterobactin to acquire free or chelated iron. These data also suggest that the deletion of *ahpC* does not interfere with transporting or utilizing siderophores or free iron and that AhpC has a specific role in enterobactin biosynthesis or secretion rather than a general role in iron metabolism.

AhpC participates in 2,3-dihydroxybenzoic acid production. Enterobactin biosynthesis in *E. coli* can be divided into two main stages: the early steps lead to the synthesis of DHB, and later reactions produce enterobactin from DHB and serine (50) (Fig. 1). The amount of DHB produced can be estimated by the Arnow assay using an *entF* mutant, which is blocked in the conversion of DHB to enterobactin. The results of the Arnow assay showed a significant reduction in catechols secreted by the *ahpC entF* double mutant compared to the *entF* strain in T medium (100 ± 29 Arnow units and 183 ± 66 Arnow units, respectively) ($P < 0.05$ by Student's *t* test), indicating that deletion of *ahpC* led to a reduction in the production of the catechol DHB. The intermediate product DHB was also tested for the ability to suppress the increased EDDA sensitivity of the *ahpC* mutant. Supplying the *ahpC* mutant with DHB enabled the mutant to grow to the same level as the wild-type strain under iron-limiting conditions (Fig. 8A). These results suggested that AhpC participates in the early stage of enterobactin biosynthesis. This was further supported by the observation that introducing a plasmid carrying the *entABC* genes was able to suppress the increased EDDA sensitivity of the *ahpC* mutant, while a plasmid carrying *entF* did not (Fig. 8B). Thus, increasing the copy number of genes involved in the early stage of enterobactin biosynthesis suppressed the deleterious effects of the *ahpC* mutant on growth in low-iron medium.

To determine which gene or genes of the *entABC* cluster were needed to suppress the *ahpC* mutant phenotype, plasmids carrying only the *entC* gene, encoding the isochorismate synthase for conversion of chorismate to isochorismate (28), or *entAB*, encoding the enzymes for making DHB from isochorismate (27, 44), were constructed and tested in the EDDA sensitivity assay. A plasmid carrying only the *entC* gene was able to suppress the increased EDDA sensitivity of the *ahpC* mutant, while a plasmid carrying *entAB* failed to do so (Fig. 8B). Thus, enhanced expression of *entC* was sufficient to suppress the effect of the *ahpC* mutation. This suggests that AhpC participates in enterobactin biosynthesis via EntC, which is the first enzyme in the enterobactin biosynthesis pathway.

Providing extra copies of *entC* suppressed the increased EDDA sensitivity of the *ahpC* mutant grown in rich medium containing EDDA. However, the *ahpC* mutant carrying *entC* on a plasmid still showed reduced growth compared to that of the wild type in minimal medium (Fig. 9A). Because the substrate for EntC is chorismate, which is also the precursor for other aromatic compounds in the cell (9), it appeared likely that increased competition for chorismate due to synthesis of aromatic amino acids and vitamins in minimal medium could reduce the amount of chorismate available to EntC. To determine whether the reduced synthesis of enterobactin could be alleviated by reducing competition for chorismate in minimal medium, a mixture of the aromatic amino acids and *para*-aminobenzoate, all of which are synthesized from cho-

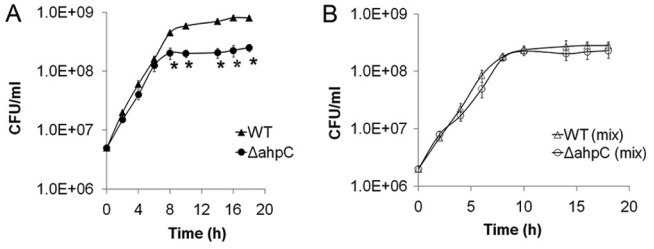

FIG 7 The *ahpC* mutant competed equally well with the wild type *in vitro*. The wild-type (BW25113) and *ahpC* (ML100) strains were grown separately (A) or in a 1:1 mix (B) in T medium, and the numbers of each strain were determined by dilution and plating at the indicated times. Data presented are averages for three measurements, and the significance of differences was determined by Student's *t* test. *, $P < 0.01$ for the *ahpC* mutant alone compared to the wild type.

TABLE 3 The *ahpC* mutant showed no defect in use of iron sources

Strain	Diam of growth zone around iron source (mm)[a]			
	E. coli[b]	Ent[c]	Fc[d]	Fe[e]
entF mutant (BW25113*entF*)	32 ± 1	20 ± 1	22 ± 2	15 ± 1
ahpC entF mutant (ML300)	31 ± 2	20 ± 1	22 ± 2	13 ± 3

[a] Data are averages ± 1 standard deviation for at least three independent experiments.
[b] Five microliters containing 10^9 cells/ml BW25113 as a source of enterobactin and related catechols.
[c] Five microliters of 10 μM purified enterobactin.
[d] Five microliters of 0.8 mM ferrichrome.
[e] Five microliters of 25 mM $FeSO_4$.

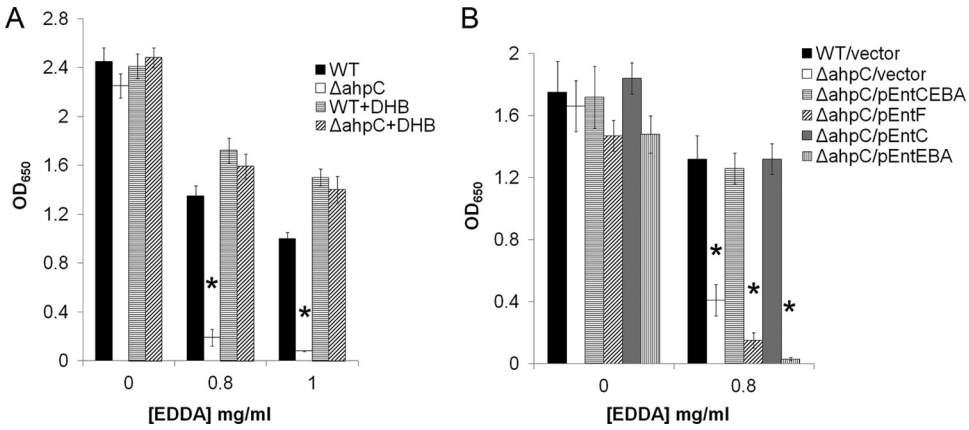

FIG 8 DHB and *entC* suppressed the increased EDDA sensitivity of the *ahpC* mutant. The strains were grown in LB broth containing EDDA for 8 h, and the OD_{650} was measured. Data presented are averages for at least three independent experiments, and error bars represent 1 standard deviation. *, $P < 0.01$ compared to the wild type, determined by Student's *t* test. (A) The wild-type (BW25113) and *ahpC* mutant (ML100) strains were grown in medium containing EDDA, with or without 1 mM DHB. (B) The wild-type strain (BW25113) carrying the empty vector (pWSK29) and the *ahpC* mutant (ML100) carrying the empty vector (pWSK29), *entCEBA* (pEnt1), *entF* (pJS4700), *entC* (pEnt2), or *entEBA* (pCP410) were grown in LB broth containing appropriate antibiotics and with or without EDDA.

rismate, was added to T medium. Adding these compounds to the minimal medium allowed the *ahpC* mutant, with (Fig. 9B) or without (data not shown) *entC* on a plasmid, to grow to the wild-type level. However, adding the amino acids individually did not support full growth of the mutant (data not shown).

Addition of the amino acids and *para*-aminobenzoate increased the amounts of extracellular catechols in both the wild-type and *ahpC* strains (Table 4). The presence of the *entC* plasmid also increased the amounts of extracellular catechols produced in both the wild-type and mutant strains, and there was an additive effect when there was both supplementation and the presence of *entC* on a plasmid (Table 4). In each of these cases, the amount of catechol secreted by the *ahpC* mutant was comparable to that for the wild type. Thus, the reduced siderophore production by the *ahpC* mutant in minimal medium is suppressed when it has more copies of *entC* or when competition of EntC for its substrate is reduced. Additionally, providing the *ahpC* mutant with the chorismate precursor shikimate restored wild-type growth to the *ahpC* mutant in the EDDA sensitivity assay (Fig. 10). Taken together, these data indicate that AhpC may participate in DHB synthesis through increasing the availability of chorismate or increasing the efficiency with which EntC uses chorismate, roles that were not anticipated given its characterization as a peroxidase.

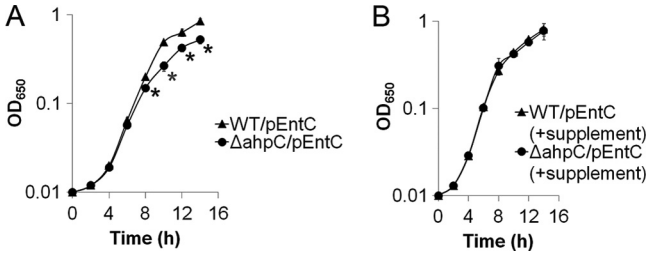

FIG 9 Supplying a mixture of aromatic amino acids and *para*-aminobenzoate suppressed the growth defect of the *ahpC* mutant in T medium. The wild-type (BW25113) and *ahpC* (ML100) strains carrying *entC* (pEnt2) were grown in T medium (A) or T medium supplemented with a mixture of aromatic amino acids and *para*-aminobenzoate (B), and growth was monitored by measuring the OD_{650} over 14 h. Data presented are averages for at least three independent experiments, and error bars represent 1 standard deviation. *, $P < 0.01$ compared to the wild type, determined by Student's *t* test.

C46 and C165 are both required for the role of AhpC in cellular iron metabolism. AhpC belongs to the 2-Cys peroxiredoxin family and has cysteines at positions 46 and 165. It has been shown that a C46S mutation of AhpC abolishes its peroxidase activity *in vitro*, while a C165S mutant maintains wild-type activity (11). In contrast, the ability of AhpC* to generate reduced glutathiones depends on C165 but not C46; the C165S mutation in AhpC* abolishes its ability to suppress the loss of Gor and TrxB, but the C46S mutation has no effect on suppression (11, 55). To determine whether either of these cysteine residues is important for AhpC to play a role in cellular iron metabolism, plasmids encoding $AhpC^{C46S}$ and $AhpC^{C165S}$ were constructed. Western blot analysis confirmed that the proteins were produced at the same level as wild-type AhpC expressed from a plasmid (Fig. 3). The plasmids containing the cysteine mutations were tested for the ability to complement the *ahpC* deletion for growth under iron-limiting conditions, and the results showed that mutation of either C46 or C165 in AhpC resulted in an increased EDDA-sensitive phenotype (Fig. 11). This indicated that both cysteine residues are important for AhpC's role in cellular iron metabolism. Analysis of the peroxide sensitivity of strains carrying the cysteine mu-

TABLE 4 Supplying aromatic amino acids and *para*-aminobenzoate or extra copies of *entC* restored wild-type levels of catechol production in the *ahpC* mutant

Strain	Catechol production[a]			
	No additions	With supplements	With pEntC	With supplements and pEntC
Wild type (BW25113)	31 ± 9	151 ± 34	125 ± 40	245 ± 25
ahpC mutant (ML100)	16 ± 3[b]	221 ± 12	138 ± 9	254 ± 20

[a] Strains carrying the empty vector or the *entC* plasmid pEnt2 (pEntC) were grown in T medium or T medium supplemented with a mixture of Trp, Tyr, Phe, and *para*-aminobenzoate (supplements). Data are expressed in Arnow units and are averages ± 1 standard deviation for at least three independent experiments.
[b] $P < 0.05$ compared to the wild type, determined by Student's *t* test.

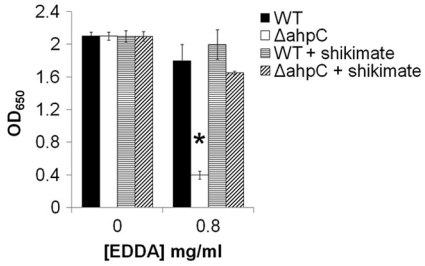

FIG 10 Shikimate suppressed the increased EDDA sensitivity of the *ahpC* mutant. Strains used were the wild-type (BW25113) and *ahpC* (ML100) strains. The strains were grown in LB broth containing EDDA, with or without 200 μM shikimate, for 8 h, and the OD_{650} was measured. Data presented are means for at least three independent experiments, and error bars represent 1 standard deviation. *, $P < 0.01$ compared to the wild type, determined by Student's *t* test.

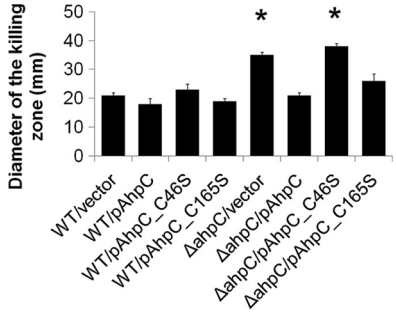

FIG 12 Resistance to cumene hydroperoxide requires AhpC C46 but not C165. Strains used were the wild-type (BW25113) and *ahpC* (ML100) strains carrying empty vector (pWSK29), *ahpC* (pAhpC), $ahpC^{C46S}$ ($pAhpC^{C46S}$), or $ahpC^{C165S}$ ($pAhpC^{C165S}$). Data are expressed in mm and are means for at least three independent experiments ± 1 standard deviation. *, $P < 0.01$ compared to the wild type, determined by Student's *t* test.

tations confirmed that the C164S mutant had peroxidase activity and was resistant to cumene hydroperoxide, while the C46S mutant was as sensitive as the *ahpC* deletion mutant to the compound (Fig. 12). The fact that both cysteines are required for participation of AhpC in cellular iron metabolism suggests that the peroxidase activity of AhpC is not sufficient for AhpC to participate in cellular iron metabolism.

DISCUSSION

In *E. coli*, it has been shown that AhpC detoxifies peroxides, is produced at high levels, and exhibits broad substrate specificity (26, 37). The expression level of AhpC is the same during aerobic and anaerobic growth at physiological pH (3). It also has been shown that the peroxidase catalytic efficiency of AhpC is not as great as that of glutathione peroxidase (37, 53). The abundance and broad specificity of AhpC could be evolutionary adaptations to compensate for its moderate peroxidase activity. However, it is also possible that AhpC participates in other cellular events that require such abundance or broad substrate specificity. It has been shown that *ahpC* can undergo mutation to *ahpC**, which encodes a protein that gains a new function to generate reduced glutathione in the absence of the Gor or TrxB cellular reductase (40). In

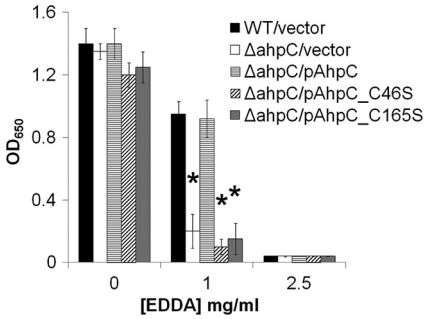

FIG 11 AhpC Cys residues 46 and 165 were both required for resistance to EDDA. The strains used were the wild-type (BW25113) and *ahpC* mutant (ML100) strains carrying the empty vector (pWSK29), *ahpC* (pAhpC), $ahpC^{C46S}$ ($pAhpC^{C46S}$), or $ahpC^{C165S}$ ($pAhpC^{C165S}$). The OD_{650} was measured after 8 h of growth in LB broth containing ampicillin and with or without EDDA. Data presented are averages for at least three independent experiments, and error bars represent 1 standard deviation. The EDDA sensitivity of ML100 carrying different plasmids was compared to that of the wild type by Student's *t* test (*, $P < 0.01$).

Streptococcus agalactiae, AhpC has been shown to serve as an intracellular chaperone for heme to optimize its trafficking and transfer to cellular targets such as catalases (25). In mammalian cells, peroxiredoxins are reported to control cytokine-induced peroxide levels that mediate signal transduction (12). These findings imply that AhpC may have diverse functionalities or be involved in multiple cellular events in *E. coli*.

The data presented in this work provide evidence that AhpC participates in cellular iron metabolism of *E. coli*. The role for AhpC in cellular iron metabolism is indicated by its reduced growth in iron-limiting medium. Under low-iron conditions, the *ahpC* mutant had a lower internal iron level and a reduction of total cellular iron content. These phenotypes correlated with a reduced production of the siderophore enterobactin in the *ahpC* mutant. The reduced secretion of DHB by the *entF ahpC* mutant and the ability to suppress the growth defect in the *ahpC* mutant by either the addition of exogenous DHB or the introduction of a plasmid carrying the *entC* gene indicated that the defect was in an early step in enterobactin biosynthesis. A mixture of aromatic amino acids and *para*-aminobenzoate, all of which were synthesized from chorismate, suppressed both the growth defect and the catechol production of the *ahpC* mutant in minimal medium. This suggests that AhpC either facilitates the delivery of the substrate chorismate to the enterobactin biosynthesis pathway or helps maintain an optimal concentration of chorismate inside *E. coli* cells.

It is possible that AhpC is required to maintain chorismate availability to the enterobactin biosynthesis pathway. Chorismate is used in the biosynthesis of many aromatic compounds, including the aromatic amino acids and folate, so multiple enzymes must compete for chorismate (9). Based on their K_m values for chorismate, these enzymes can be divided into three groups: the strong competitor group, with K_m values between 1 and 10 μM; the medium competitor group, with K_m values between 10 and 100 μM; and the weak competitor group, with K_m values of >100 μM. With a K_m value of 14 μM, EntC falls into the medium competitor group (28). If the deletion of *ahpC* leads to a reduction of the chorismate pool or a less efficient shuttling of chorismate to EntC, EntC might be at a disadvantage in competing for chorismate compared with some of the strong competitors, such as the aminodeoxychorismate synthase of the Trp biosynthesis pathway, given the relatively high K_m value of EntC for chorismate. This

competitive disadvantage would lead to a lowered production of DHB and enterobactin, causing reduced growth under iron-limiting conditions, a smaller intracellular ferrous iron pool, and a lowered total cellular iron content in the *ahpC* mutant. Providing the *ahpC* mutant with extra copies of *entC* might help EntC to compete for the limited chorismate pool. Additionally, providing the *ahpC* mutant with exogenous DHB or iron would bypass the requirement for the precursor chorismate, and supplementing shikimate or the mixture of aromatic amino acids and *para*-aminobenzoate would increase the available chorismate concentration for the enterobactin biosynthesis pathway.

The peroxidase activity of AhpC may contribute to the efficiency of enterobactin production if EntC or the chorismate pool is very sensitive to peroxide. A recent report (18) showed that under peroxide stress, a small RNA (sRNA), RybA, downregulates aromatic amino acid biosynthesis, and the authors of that report suggest that this may increase the availability of chorismate to other biosynthetic pathways. Waters et al. (52) observed that this gene encodes a small protein, which they designated MntS. They noted an increase in *entC* expression in an MntR mutant, which overexpressed the MntS sRNA, when the cells were grown with a high manganese concentration. These data indicate a link between peroxide stress, the chorismate pool, and enterobactin gene expression. However, in the absence of other factors, these observations would predict that peroxide stress such as that induced by the *ahpC* mutation would increase the availability of chorismate for EntC and also increase enterobactin biosynthesis. Thus, AhpC would appear to have an effect in addition to its role in reducing peroxide in the cell.

Additional evidence that the peroxidase activity of AhpC is not solely responsible for AhpC's participation in cellular iron metabolism is seen in the requirement for both cysteine residues. The C146S mutant had peroxidase activity and was resistant to cumene hydroperoxide, but it failed to support wild-type growth under iron-limiting conditions.

The fact that *ahpC** on a plasmid was not able to suppress the *ahpC* mutant phenotype suggests that the ability to generate reduced glutathione is not important for AhpC's participation in cellular iron metabolism. Thus, AhpC's participation in cellular iron metabolism is a new role of AhpC. This undesignated role of AhpC provides, for the first time, an example of a peroxiredoxin participating in a cellular process other than detoxifying peroxides in *E. coli*, which expands the versatility of peroxiredoxins in prokaryotes.

Although increasing the copy number of *entC* in the cell compensated for the loss of *ahpC*, it is unlikely that AhpC enhances the enzymatic activity of EntC or is involved in the recycling of an EntC cofactor. The crystal structure of EntC (46) with bound isochorismate indicates that the catalytic center contains a magnesium ion and the isochorismate product, but no cofactor, such as flavin adenine dinucleotide (FAD) or flavin mononucleotide (FMN), has been found to participate in EntC's catalytic reaction (28, 46). There is no indication that EntC forms any inter- or intramolecular disulfide bonds or catalyzes any oxidation-reduction reaction (28, 46). It has been shown that the function of the chorismate synthase in *E. coli* requires reduced FMN, but the NADPH:FMN oxidoreductase that provides the cofactor has not been identified (30). Since AhpC catalyzes oxidation-reduction reactions, and as both of its cysteine residues are important for its participation in cellular iron metabolism of *E. coli*, AhpC may participate in the reduction of FMN for chorismate synthesis, either directly or indirectly. This participation would enable AhpC to influence cellular chorismate levels, which would offset multiple pathways, including enterobactin biosynthesis. However, further studies are needed to elucidate these possibilities.

ACKNOWLEDGMENTS

This work was supported by grants AI091957 and AI16935 from the National Institutes of Health.

We thank George Georgiou for providing strains DHB4 and SMG96, Leslie B. Poole for providing the anti-AhpC antibody, the National BioResource Project (NIG, Japan) for providing *E. coli* Keio mutant strains, Nathan Miller for performing ICP-MS, and Marvin Mercado for performing LC-MS. Alexandra Mey provided assistance with the real-time PCR analysis and review of the manuscript. We thank Elizabeth Wyckoff and other members of the laboratory for critical reviews of the manuscript and for helpful discussions.

REFERENCES

1. **Arnow EL.** 1937. Colorimetric determination of the components of 3,4-dihydroxyphenylalanine-tyrosine mixtures. J. Biol. Chem. **1937**: 531–537.
2. **Baba T, et al.** 2006. Construction of *Escherichia coli* K-12 in-frame, single-gene knockout mutants: the Keio collection. Mol. Syst. Biol. **2**:2006.0008. doi:10.1038/msb4100050.
3. **Blankenhorn D, Phillips J, Slonczewski JL.** 1999. Acid- and base-induced proteins during aerobic and anaerobic growth of *Escherichia coli* revealed by two-dimensional gel electrophoresis. J. Bacteriol. **181**:2209–2216.
4. **Braun V.** 2003. Iron uptake by *Escherichia coli*. Front. Biosci. **8**:1409–1421.
5. **Braun V, Braun M, Killmann H.** 2004. Ferrichrome- and citrate-mediated iron transport, p 158–177. *In* Crosa JH, Mey AR, Payne SM (ed), Iron transport in bacteria. ASM Press, Washington, DC.
6. **Carmel-Harel O, Storz G.** 2000. Roles of the glutathione- and thioredoxin-dependent reduction systems in the *Escherichia coli* and *Saccharomyces cerevisiae* responses to oxidative stress. Annu. Rev. Microbiol. **54**: 439–461.
7. **Crosa JH, Walsh CT.** 2002. Genetics and assembly line enzymology of siderophore biosynthesis in bacteria. Microbiol. Mol. Biol. Rev. **66**:223–249.
8. **Datsenko KA, Wanner BL.** 2000. One-step inactivation of chromosomal genes in *Escherichia coli* K-12 using PCR products. Proc. Natl. Acad. Sci. U. S. A. **97**:6640–6645.
9. **Dosselaere F, Vanderleyden J.** 2001. A metabolic node in action: chorismate-utilizing enzymes in microorganisms. Crit. Rev. Microbiol. **27**:75–131.
10. **Ehmann DE, Shaw-Reid CA, Losey HC, Walsh CT.** 2000. The EntF and EntE adenylation domains of *Escherichia coli* enterobactin synthetase: sequestration and selectivity in acyl-AMP transfers to thiolation domain cosubstrates. Proc. Natl. Acad. Sci. U. S. A. **97**:2509–2514.
11. **Ellis HR, Poole LB.** 1997. Roles for the two cysteine residues of AhpC in catalysis of peroxide reduction by alkyl hydroperoxide reductase from *Salmonella typhimurium*. Biochemistry **36**:13349–13356.
12. **Farhana L, et al.** 2004. Apoptosis signaling by the novel compound 3-Cl-AHPC involves increased EGFR proteolysis and accompanying decreased phosphatidylinositol 3-kinase and AKT kinase activities. Oncogene **23**:1874–1884.
13. **Farinha MA, Kropinski AM.** 1990. Construction of broad-host-range plasmid vectors for easy visible selection and analysis of promoters. J. Bacteriol. **172**:3496–3499.
14. **Faulkner MJ, Veeravalli K, Gon S, Georgiou G, Beckwith J.** 2008. Functional plasticity of a peroxidase allows evolution of diverse disulfide-reducing pathways. Proc. Natl. Acad. Sci. U. S. A. **105**:6735–6740.
15. **Freedman HH, Frost AE, Westerback SJ, Martell AE.** 1957. Chelating tendencies of N,N′-ethylenebis-[2-(o-hydroxyphenyl)]glycine. Nature **179**:1020–1021.
16. **Furrer JL, Sanders DN, Hook-Barnard IG, McIntosh MA.** 2002. Export of the siderophore enterobactin in *Escherichia coli*: involvement of a 43 kDa membrane exporter. Mol. Microbiol. **44**:1225–1234.

17. **Gehring AM, Bradley KA, Walsh CT.** 1997. Enterobactin biosynthesis in *Escherichia coli*: isochorismate lyase (EntB) is a bifunctional enzyme that is phosphopantetheinylated by EntD and then acylated by EntE using ATP and 2,3-dihydroxybenzoate. Biochemistry **36**:8495–8503.
18. **Gerstle K, Klätschke K, Hahn U, Piganeau N.** 2012. The small RNA RybA regulates key-genes in the biosynthesis of aromatic amino acids under peroxide stress in *E. coli*. RNA Biol. **9**:458–468.
19. **Goldberg JB, Ohman DE.** 1984. Cloning and expression in *Pseudomonas aeruginosa* of a gene involved in the production of alginate. J. Bacteriol. **158**:1115–1121.
20. **Hantke K.** 1981. Regulation of ferric iron transport in *Escherichia coli* K12: isolation of a constitutive mutant. Mol. Gen. Genet. **182**:288–292.
21. **Ho SN, Hunt HD, Horton RM, Pullen JK, Pease LR.** 1989. Site-directed mutagenesis by overlap extension using the polymerase chain reaction. Gene **77**:51–59.
22. **Jönsson TJ, Ellis HR, Poole LB.** 2008. Cysteine reactivity and thiol-disulfide interchange pathways in AhpF and AhpC of the bacterial alkyl hydroperoxide reductase system. Biochemistry **46**:5709–5721.
23. **Klebba PE.** 2003. Three paradoxes of ferric enterobactin uptake. Front. Biosci. **8**:1422–1436.
24. **Kolter R, Inuzuka M, Helinski DR.** 1978. Trans-complementation-dependent replication of a low molecular weight origin fragment from plasmid R6K. Cell **15**:1199–1208.
25. **Lechardeur D, et al.** 2010. The 2-Cys peroxiredoxin alkyl hydroperoxide reductase c binds heme and participates in its intracellular availability in *Streptococcus agalactiae*. J. Biol. Chem. **285**:16032–16041.
26. **Link AJ, Robison K, Church GM.** 1997. Comparing the predicted and observed properties of proteins encoded in the genome of *Escherichia coli* K-12. Electrophoresis **18**:1259–1313.
27. **Liu J, Duncan K, Walsh CT.** 1989. Nucleotide sequence of a cluster of *Escherichia coli* enterobactin biosynthesis genes: identification of *entA* and purification of its product 2,3-dihydro-2,3-dihydroxybenzoate dehydrogenase. J. Bacteriol. **171**:791–798.
28. **Liu J, Quinn N, Berchtold GA, Walsh CT.** 1990. Overexpression, purification, and characterization of isochorismate synthase (EntC), the first enzyme involved in the biosynthesis of enterobactin from chorismate. Biochemistry **29**:1417–1425.
29. **Lorenzo V, Perez-Martin J, Escolar L, Pesole G, Bertoni G.** 2004. Mode of binding of the Fur protein to target DNA: negative regulation of iron-controlled gene expression, p 185–196. *In* Crosa JH, Mey AR, Payne SM (ed), Iron transport in bacteria. ASM Press, Washington, DC.
30. **Macheroux P, Schmid E, Amrhein N, Schaller A.** 1999. A unique reaction in a common pathway: mechanism and function of chorismate synthase in the shikimate pathway. Planta **207**:325–334.
31. **Mey AR, Payne SM.** 2001. Haem utilization in *Vibrio cholerae* involves multiple TonB-dependent haem receptors. Mol. Microbiol. **42**:835–849.
32. **Mey AR, Craig SA, Payne SM.** 2005. Characterization of *Vibrio cholerae* RyhB: the RyhB regulon and role of ryhB in biofilm formation. Infect. Immun. **73**:5706–5719.
33. **Mey AR, Wyckoff EE, Hoover LA, Fisher CR, Payne SM.** 2008. *Vibrio cholerae* VciB promotes iron uptake via ferrous iron transporters. J. Bacteriol. **190**:5953–5962.
34. **Miller JH.** 1972. Experiments in molecular genetics, p 352–355. Cold Spring Harbor Laboratory Press, Cold Spring Harbor, NY.
35. **Neilands JB.** 1995. Siderophores: structure and function of microbial iron transport compounds. J. Biol. Chem. **270**:26723–26726.
36. **O'Brien IG, Gibson F.** 1970. The structure of enterochelin and related 2,3-dihydroxy-N-benzoylserine conjugates from *Escherichia coli*. Biochim. Biophys. Acta **215**:393–402.
37. **Parsonage D, Karplus PA, Poole LB.** 2008. Substrate specificity and redox potential of AhpC, a bacterial peroxiredoxin. Proc. Natl. Acad. Sci. U. S. A. **105**:8209–8214.
38. **Pickett CL, Hayes L, Earhart CF.** 1984. Molecular cloning of the *Escherichia coli* K-12 *entACGBE* genes. FEMS Microbiol. Lett. **24**:77–80.
39. **Pollack JR, Neilands JB.** 1970. Enterobactin, an iron transport compound from *Salmonella typhimurium*. Biochem. Biophys. Res. Commun. **38**:989–992.
40. **Ritz D, Lim J, Reynolds CM, Poole LB, Beckwith J.** 2001. Conversion of a peroxiredoxin into a disulfide reductase by a triplet repeat expansion. Science **294**:158–160.
41. **Ritz D, Beckwith J.** 2001. Roles of thiol-redox pathways in bacteria. Annu. Rev. Microbiol. **55**:21–48.
42. **Rogers HJ.** 1973. Iron-binding catechols and virulence in *Escherichia coli*. Infect. Immun. **7**:445–456.
43. **Runyen-Janecky LJ, Hong M, Payne SM.** 1999. The virulence plasmid-encoded *impCAB* operon enhances survival and induced mutagenesis in *Shigella flexneri* after exposure to UV radiation. Infect. Immun. **67**:1415–1423.
44. **Rusnak F, Liu J, Quinn N, Berchtold GA, Walsh CT.** 1990. Subcloning of the enterobactin biosynthetic gene *entB*: expression, purification, characterization, and substrate specificity of isochorismatase. Biochemistry **29**:1425–1435.
45. **Simon EH, Tessman I.** 1963. Thymidine requiring mutants of phage T4. Proc. Natl. Acad. Sci. U. S. A. **50**:526–532.
46. **Sridharan S, et al.** 2010. Crystal structure of *Escherichia coli* enterobactin-specific isochorismate synthase (EntC) bound to its reaction product isochorismate: implications for the enzyme mechanism and differential activity of chorismate-utilizing enzymes. J. Mol. Biol. **397**:290–300.
47. **Staab JF.** 1990. Studies on the *Escherichia coli* enterobactin synthetase. Ph.D. thesis. The University of Texas, Austin, TX.
48. **Tartaglias LA, Storz G, Brodsky MH, Lai A, Ames BN.** 1990. Alkyl hydroperoxide reductase from *Salmonella typhimurium*. Sequence and homology to thioredoxin reductase and other flavoprotein disulfide oxidoreductases. Biochemistry **265**:10535–10540.
49. **Walsh CT, Liu J, Rusnak F, Sakaitani M.** 1990. Molecular studies on enzymes in chorismate metabolism and the enterobactin biosynthetic pathway. Chem. Rev. **1990**:1105–1129.
50. **Walsh CT, Marshall GC.** 2004. Siderophore biosynthesis in bacteria, p 18–37. *In* Crosa JH, Mey AR, Payne SM (ed), Iron transport in bacteria. ASM Press, Washington, DC.
51. **Wang R, Kushner S.** 1991. Construction of versatile low-copy-number vectors for cloning, sequencing and gene expression in *Escherichia coli*. Gene **100**:195–199.
52. **Waters LS, Sandoval M, Storz G.** 2011. The *Escherichia coli* MntR miniregulon includes genes encoding a small protein and an efflux pump required for manganese homeostasis. J. Bacteriol. **193**:5887–5897.
53. **Wood ZA, Schröder E, Robin Harris J, Poole LB.** 2003. Structure, mechanism and regulation of peroxiredoxins. Trends Biochem. Sci. **28**:32–40.
54. **Wyckoff EE, Smith SL, Payne SM.** 2001. VibD and VibH are required for late steps in vibriobactin biosynthesis in *Vibrio cholerae*. J. Bacteriol. **183**:1830–1834.
55. **Yamamoto Y, et al.** 2008. Mutant AhpC peroxiredoxins suppress thiol-disulfide redox deficiencies and acquire deglutathionylating activity. Mol. Cell **29**:36–45.